

PHY 564

Advanced Accelerator Physics

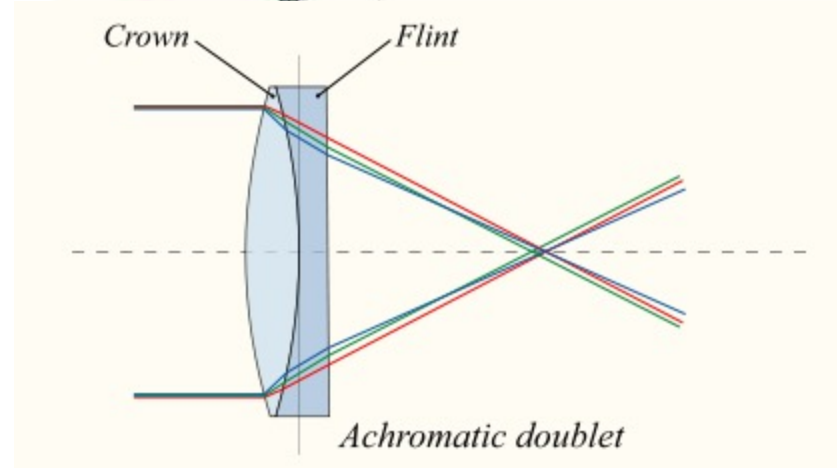
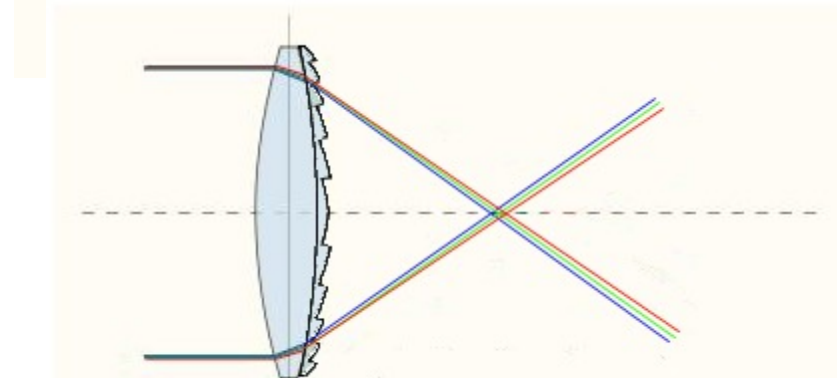
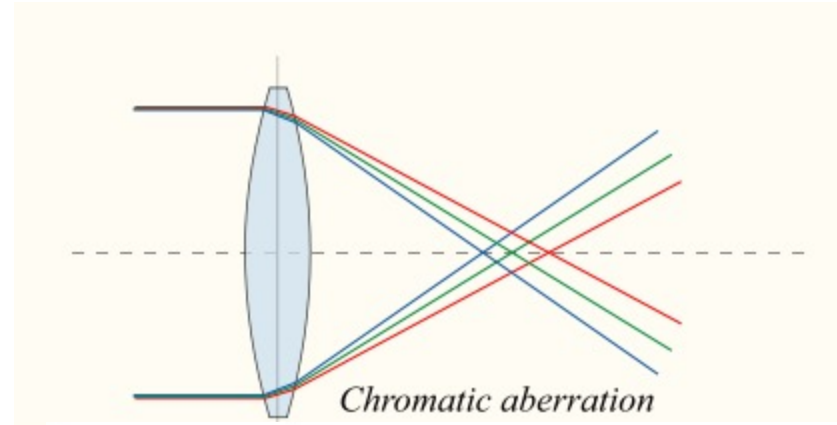
Lecture 23

Nonlinear elements and nonlinear dynamics. Part I

Vladimir N. Litvinenko

CENTER for ACCELERATOR SCIENCE AND EDUCATION
Department of Physics & Astronomy, Stony Brook University

Chromaticity and correction



Nonlinear effects in particle's motion arise from various sources: high order kinematic terms in Hamiltonian expansion, spatial and temporal inhomogeneity of EM fields, edge effects, bending (e.g. bending plus gradient generates third order term), collective fields (space charge, wake-fields, beam-beam collisions). Typical methods include Hamiltonian perturbation methods or numerical tracking of many types (from particles tracking to particle-in-cell codes). A novel approach, exploiting symmetries of Hamiltonian systems and power of Lie algebraic tools, is the most comprehensive approach to the non-linear beam dynamics. Hence, a short introduction to this method.

But first, let us start by discussing a typical – and very important – nonlinear effect called chromaticity. It is nothing else than dependence of the betatron tune on particle's energy. While you can do this for fully coupled motion using our well-developed parameterization and perturbation methods, here –for compactness - we will consider just an uncoupled betatron motion with Hamiltonian in transverse magnetic field:

$$\tilde{h} = -P_s = -(1 + Kx)\sqrt{p^2 - p_x^2 - p_y^2} + \frac{e}{c}A_s; \quad p = p_o(1 + \delta);$$

$$\frac{d(x,y)}{ds} = \frac{\partial \tilde{h}}{\partial p_{x,y}} = -(1 + Kx)\frac{p_{x,y}}{\sqrt{p^2 - p_x^2 - p_y^2}} \cong -(1 + Kx)\frac{p_{x,y}}{p_o(1 + \delta)} + O(p_{x,y}^3); \quad (1)$$

$$\frac{dp_x}{ds} = -\frac{\partial \tilde{h}}{\partial x} = K\sqrt{p^2 - p_x^2 - p_y^2} - \frac{e}{c}\frac{\partial A_s}{\partial x}; \quad \frac{dp_y}{ds} = -\frac{\partial \tilde{h}}{\partial y} = -\frac{e}{c}\frac{\partial A_s}{\partial y};$$

with

$$A_2 = \sum_{n=1}^{\infty} \left\{ \partial_x^{n-1} \left((1 + Kx) B_y \right) \frac{x^n}{n!} - \partial_y^{n-1} \left((1 + Kx) B_x \right) \frac{y^n}{n!} \right\} \quad (2)$$

If we consider easiest scenario for a storage ring using pure dipole and quadrupole field we get:

$$\frac{eA_z}{c} = \frac{eB_y}{c}x + \frac{eG}{c} \frac{x^2 - y^2}{2} + p_o K^2 \frac{x^2}{2}; \quad K = \frac{eB_{yro}}{p_o c}. \quad (3)$$

expression which does not contain any nonlinear terms (cubic or higher). Remember that linear term in (3) disappears because of the condition on the reference orbit. We can see that angle is x', y' inverse proportional to the particle's momentum $p = p_o(1 + \delta)$ while the force $p'_{x,y}$ does not depend on the particle's momentum. Hence, the lowest order (cubic) term in the Hamiltonian expansion are $\delta \cdot p_{x,y}^2$.

Since here we are considering constant energy of our particles ($p = \text{const}$) and betatron oscillations, we also can rewrite (1) in more traditional form

$$h = -(1 + Kx) \sqrt{1 - \pi_x^2 - \pi_y^2} + \frac{e}{pc} A_s(x, y, s); \quad \pi_{x,y} = \frac{p_{x,y}}{p} = \frac{p_{x,y}}{p_o(1 + \delta)};$$

$$\frac{d(x, y)}{ds} = \frac{\partial h}{\partial \pi_{x,y}} = -(1 + Kx) \frac{\pi_{x,y}}{\sqrt{1 - \pi_x^2 - \pi_y^2}} \cong -(1 + Kx) \pi_{x,y} + O(\pi_{x,y}^3) \quad (4)$$

$$\frac{d\pi_{x,y}}{ds} = -\frac{\partial h}{\partial(x, y)} = -\frac{e}{pc} \frac{\partial A_s}{\partial(x, y)} = -\frac{e}{p_o c(1 + \delta)} \frac{\partial A_s}{\partial(x, y)}.$$

which clearly indicates that with fixed magnetic field, its affect on the particle is inverse proportional to particle's momentum p_o . This is traditional way of consider chromatic effect. Naturally, both descriptions are identical and gave exactly the same result! But this is always lost in description of chromatic effects that its origin is purely geometrical – for the same “so-called normalized” transverse emittance, angle of trajectory is inverse proportional to the particle's longitudinal momentum. In the Hamiltonian (4), the lowest (cubic) terms are $\delta \cdot x^2, \delta \cdot y^2$.

From our Hamiltonians it is obvious that there are nonlinear kinematic terms $\sim \pi_{x,y}^4$, $\pi_x^2 \pi_y^2$ and higher in the Hamiltonian expansion. Furthermore, there are always third order $Kx\pi_{x,y}^2$ terms. While this term can cause third order resonance (we will look at them later) its role is not as important as that of the chromaticity of betatron oscillations. Hence, let's leave in the Hamiltonian (4) only linear (up to quadratic term) for transverse motion while keeping particle momentum arbitrary:

$$H = \frac{\pi_x^2 + \pi_y^2}{2} + \frac{1}{1+\delta} \left((K_1 + K^2) \frac{x^2}{2} - K_1 \frac{y^2}{2} \right);$$

$$H = H_o + \Delta H; \quad \Delta H = -\frac{\delta}{1+\delta} \left((K_1 + K^2) \frac{x^2}{2} - K_1 \frac{y^2}{2} \right).$$
(5)

Note, that similar (but much-much longer) expression can be derived for arbitrary magnetic and electric fields. While possible, it does not bring any new physics into what we considering here.

We already found what (in first order of perturbation) the tune shift will result from variation of the Hamiltonian (using our perturbation method):

$$\Delta Q_x \cong -\frac{1}{4\pi} \frac{\delta}{1+\delta} \oint \beta_x (K_1 + K^2) ds; \quad \Delta Q_y \cong \frac{1}{4\pi} \frac{\delta}{1+\delta} \oint \beta_y K_1 ds;$$
(6)

e.g. the betatron tunes in such storage ring depend on the particle momentum (energy). Note that keeping $1+\delta$ in the denominator is overestimation of accuracy in (6) – there are other terms of order δ^2 and higher. The linear term in (6) is called chromaticity

$$C_x = \frac{\Delta Q_x}{\delta} \cong -\frac{1}{4\pi} \oint \beta_x (K_1 + K^2) ds; \quad C_y = \frac{\Delta Q_y}{\delta} \cong \frac{1}{4\pi} \oint \beta_y K_1 ds;$$
(7)

Note that the linear chromatic term is strictly speaking is result of non-linear (third order) term in the Hamiltonian. Still, there is tradition to call it linear chromaticity and call the higher orders - higher order chromaticity. One important observation is that natural chromaticity (7) usually has negative values (“focusing of higher energy particles is weaker”) for practically all storage rings. While statement in brackets is not strictly rigorous, it is true that for very high energy particles tunes will go to zero. A better explanation is coming from observation that in strong-focusing storage rings beta-functions are reaching maxima in focusing elements (e.g. β_x reaches maxima in focusing quadrupoles, while β_y reaches maxima in horizontally de-focusing quadrupoles where $K_1 < 0$) and therefore this tendency is correct. Furthermore, expectation for their values is that of the storage ring tune: $C_{x,y} \sim -(1 \div 2) \cdot Q_{x,y}$. Still, it is impossible to prove this rule explicitly in general case.

Chromaticity has multiplicity of effects on particle’s dynamics in storage rings. In modern storage rings with $Q \sim 10-100$, chromatic effects are very important. Chromaticity can generates spread of betatron tunes (for a typical energy spread $\sim 10^{-3}-10^{-4}$), which can move particles onto linear and non-linear resonances. It also can impede injection into the storage rings as dynamics aperture (e.g. limit amplitudes of stable oscillations). Hence, chromaticity is usually corrected (by sextupoles, as we discuss it later in the lecture) to few units.

But the most important problem that natural (e.g. negative) chromaticity creates is so called head-tail instability, which occurs at energies above the critical, e.g. when the slip factor is negative. Head-tail instability is one of few major menaces in storage rings, which can simply kill the beam if not taken care off.

Incomplete list of major instabilities in a storage ring:

1. Wrong lattice, where motion is unstable;
2. Robertson instability (operating RF cavities with wrong sign of frequency detuning - we are not discussing it in this course);
3. Integer and parametric resonances (and frequently 3rd and 4th order resonances);
4. Head-tail instability.

While a nasty microwave instability would fortunately saturate by inducing growth of energy spread, but not head-tail instability. It could be major killer of the beams.

Let's consider this menace using a simple two-macro-particle model, which was originally used to describe this experimentally observed phenomena. In Fig. 1 we depict this simple model when two macro-particles execute slow synchrotron oscillations 180-degrees out of phase – hence the name, head and tail: when one particle is in front of the bunch, the other is at the tail, and vice-versa.

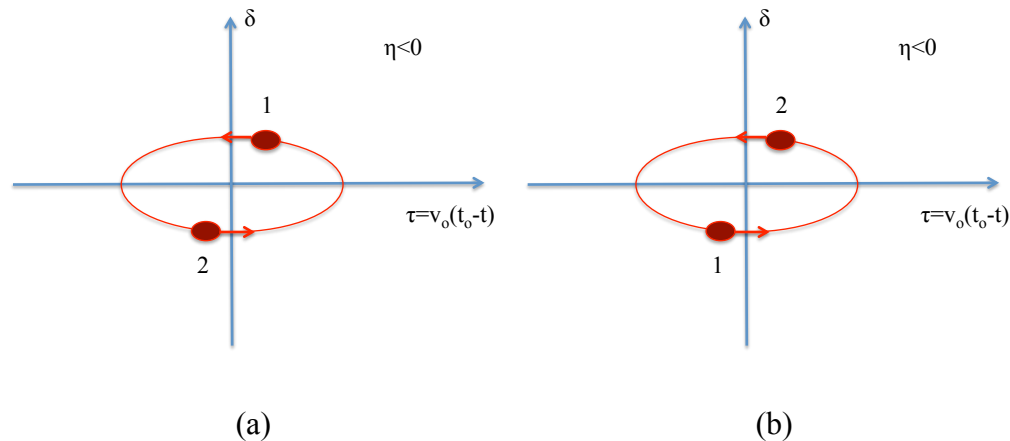
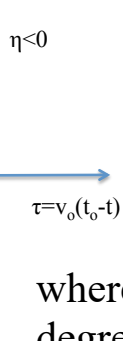


Fig. 1 Two macro-particles executing synchrotron oscillations. (a) particle 1 is in front of particles 2, (b) 180-degrees later – particles exchange the positions.

Since instability is sensitive to the chromaticity, details (such as strength of the wake-field and value of the amplitude of the oscillations) are not important. It is also an indication of universality of this problem – it just occurs if chromaticity is on a wrong sign! (e.g. negative for negative slippage). We will simply use some arbitrary values assuming that synchrotron oscillations are much slower than betatron ones. Finally, one more important fact you learned from the class on wake-fields and instabilities: particles in front of the bunch generate wake sensed by those in the tail, not vice-versa!



Hence: for the Fig. 1 (a) we can write equations of motions as (we use y as generic transverse coordinate):

$$y_1'' + K_1(s)(1 - \delta_1)y_1 = 0; \quad (7)$$

$$y_2'' + K_1(s)(1 - \delta_2)y_2 = W \cdot y_1;$$

where W is a transverse focusing (or defocusing) induced by macro-particle ahead. 180-degrees later, it changes to

$$y_1'' + K_1(s)(1 - \delta_1)y_1 = W \cdot y_2; \quad (7')$$

$$y_2'' + K_1(s)(1 - \delta_2)y_2 = 0;$$

where we just need to add

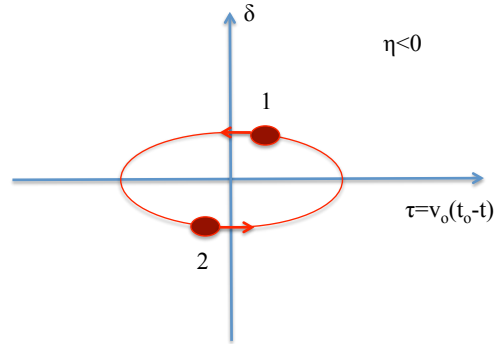
$\tau = v_0(t_0 - t)$

$$\delta_1 = \delta \cos \varphi_s; \delta_2 = -\delta \cos \varphi_s; \quad \varphi_s = \Omega_s s; \quad S = \frac{\pi}{\Omega_s};$$

$$\tau_1 = \tau \sin \varphi_s; \tau_2 = -\tau \sin \varphi_s;$$

$$y_1'' + K_1(s)(1 - \delta_1)y_1 = W \frac{1 - \text{sign}(\tau_2 - \tau_1)}{2} \cdot y_2; \quad (8)$$

$$y_2'' + K_1(s)(1 - \delta_2)y_2 = W \frac{1 + \text{sign}(\tau_2 - \tau_1)}{2} \cdot y_1;$$



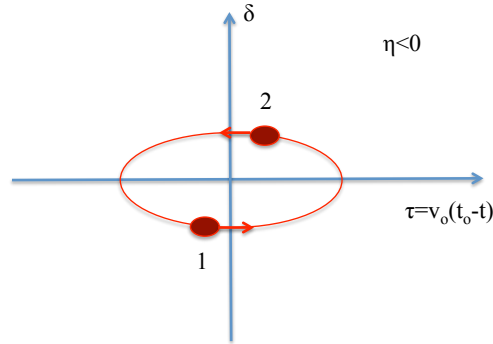
Let's consider particle (1) and (2) having complex amplitudes of oscillations a_1 and a_2 starting at zero s . For the first $\varphi_s = \{0, 180\}$ degrees in picture (a).

$$y_1 = w_y \operatorname{Re} a_{10} e^{i(\psi + \Delta\psi)}; y_2 = w_y \operatorname{Re} a_{20} e^{i(\psi - \Delta\psi)};$$

$$\Delta\psi(s) = 2\pi C_y \delta \int_0^s \cos \Omega_s s ds = \frac{2\pi C_y \delta}{\Omega_s} \sin \Omega_s s; \quad S = \frac{\pi}{\Omega_s};$$

$$a_2(s) = a_{20} + \frac{a_{10}}{2i} \int_0^s W w_y^2 e^{2i\Delta\psi} ds; \quad a_{21} = a_2(S) = a_{20} + a_{10} \langle W w_y^2 \rangle \frac{1}{2i} \int_0^S e^{2i\Delta\psi} ds; \quad (9)$$

$$\begin{pmatrix} a_1(S) \\ a_2(S) \end{pmatrix} = \begin{bmatrix} 1 & 0 \\ u & 1 \end{bmatrix} \begin{pmatrix} a_{10} \\ a_{20} \end{pmatrix}; \quad u = \langle W w_y^2 \rangle \frac{1}{2i} \int_0^S e^{2i\Delta\psi} ds.$$



Now, let's look how the amplitude of oscillation of first particles changes during next half of the synchrotron oscillation:

$$y_1 = w_y \operatorname{Re} a_1(s) e^{i(\psi - \Delta\psi)}; y_2 = w_y \operatorname{Re} a_{21} e^{i(\psi + \Delta\psi)};$$

$$a_1(s) = a_{10} + a_{21} \frac{1}{2i} \int_S^s W w_y^2 e^{2i\Delta\psi} ds; a_{11} = a_1(2S) = a_{10} + a_{21} \langle W w_y^2 \rangle \frac{1}{2i} \int_S^{2S} e^{2i\Delta\psi} ds; (10)$$

$$\begin{pmatrix} a_1(2S) \\ a_2(2S) \end{pmatrix} = \begin{bmatrix} 1 & u \\ 0 & 1 \end{bmatrix} \begin{pmatrix} a_{10} \\ a_{21} \end{pmatrix}; u = \langle W w_y^2 \rangle \frac{1}{2i} \int_0^S e^{2i\Delta\psi} ds.$$

The overall matrix for a single synchrotron oscillation period is

$$\begin{pmatrix} a_{11} \\ a_{21} \end{pmatrix} = \begin{bmatrix} 1 & u \\ 0 & 1 \end{bmatrix} \begin{bmatrix} 1 & 0 \\ u & 1 \end{bmatrix} \begin{pmatrix} a_{10} \\ a_{20} \end{pmatrix} = \begin{bmatrix} 1+u^2 & u \\ u & 1 \end{bmatrix} \begin{pmatrix} a_{10} \\ a_{20} \end{pmatrix},$$

$$\det \begin{bmatrix} 1+u^2-\lambda & u \\ u & 1-\lambda \end{bmatrix} = (1-\lambda)(1+u^2-\lambda) - u^2 = (1-\lambda)^2 - \lambda u^2; \quad (11)$$

$$\lambda_{1,2} = 1 + \frac{u^2}{2} \pm u \sqrt{1 + \frac{u^2}{4}}; u = \langle W w_y^2 \rangle \frac{1}{2i} \int_0^S e^{2i\Delta\psi} ds.$$

Note that determinant of matrix is 1, hence is one solution is growing, the other is damped. Since we are considering weak wake-field, we can write the eigen values as

$$u \approx \langle W w_y^2 \rangle \left(\frac{S}{2i} + \frac{2\pi C_y \delta}{\Omega_s} \right); \quad \lambda_{1,2} \cong e^{\pm \langle W w_y^2 \rangle \left(\frac{S}{2i} + \frac{2\pi C_y \delta}{\Omega_s} \right)} \quad (12)$$

and the growth rate is proportional to the chromaticity and its value should be limited. The detailed studies (which we have to skip) show that + (sign instability corresponding to positive chromaticity) is much weaker and that having a small positive chromaticity for storage ring above transition (negative slip factor) is required for stability of the beam – this is the mode in which most of electron storage ring and high energy hadron colliders do operate.

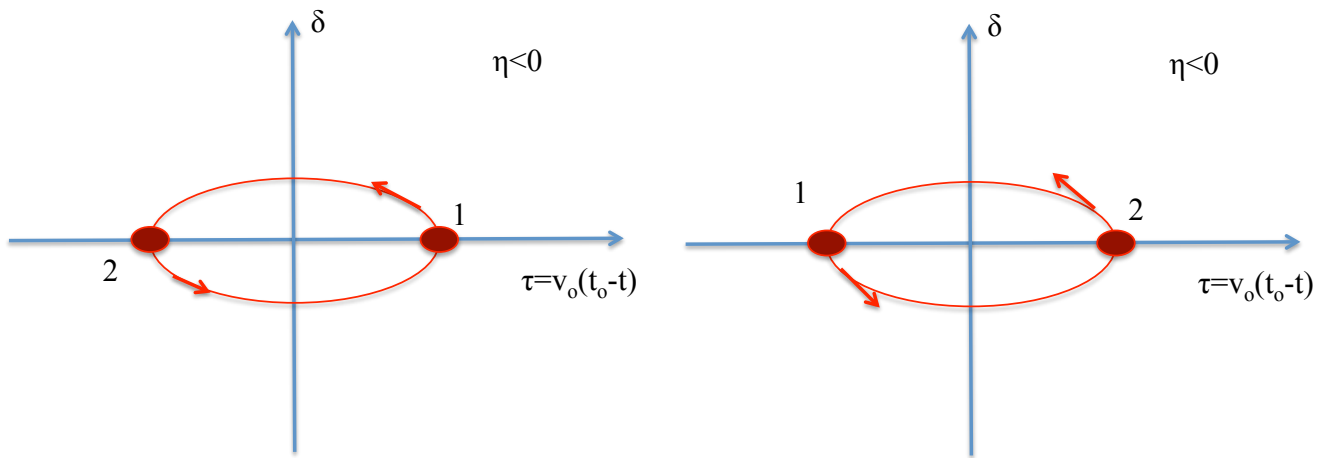


Fig.2. Two extreme positions.

Intuitively this can be described as follows. Let's consider negative chromaticity and the fact that the strength of the transverse wakefield is increasing with the distance between particles, e.g. most of the impact will come from the head particle (1) when it is in extreme forward position. (1) excites the tail particle (2) resonantly it oscillates in phase.

$$\tilde{y}_2 = \tilde{y}_{20} + T \varepsilon \tilde{y}_{10}$$

When they exchange position, the excited tail particle (2) oscillates with higher betatron frequency (it passes through lower energy) than the (1) having higher energies. It means that particle (2) comes to head position with positive phase advance – it corresponds to an effective response from the future

$$\Delta \tilde{y}_1(t) = T \varepsilon \tilde{y}_{20}(t + \tau) + T \varepsilon^2 \tilde{y}_{10}(t + \tau)$$

We can equivalently write

$$y_1''(t) + \omega^2 y_1(t) = T \varepsilon^2 \tilde{y}_1(t + \tau) \approx T \varepsilon^2 (\tilde{y}_1(t) + \tau \tilde{y}_1'(t)); \quad (13)$$

generating growth rate of $\tau T \varepsilon^2$. We should note that $\tau = -\frac{4\pi C_y \delta}{\Omega_s c}$ is proportional to the

chromaticity and has opposite sign for negative slippage. For positive slippage (below transition), natural sign of chromaticity is favored for head-tail stability.

These exercises were to establish a need for chromaticity compensations. Naturally, linear element cannot do this (they are introducing the chromaticity, not compensating it!). Hence, let's consider sextupole fields with

$$\frac{eA_2}{c} = \frac{eS}{c} \frac{x^3 - 3xy^2}{3!} \quad (14)$$

you can easily check that it satisfies 2D Maxwell equation. We are aware that in storage ring closed orbit depends on particle's momentum as

$$x_\delta = \eta_x(s)\delta \quad (15)$$

and introduction of sextupoles in (5) will result is:

$$H = \frac{\pi_x^2 + \pi_y^2}{2} + \frac{1}{1+\delta} \left((K_1 + K^2) \frac{x_\beta^2}{2} - K_1 \frac{y^2}{2} \right) + \frac{1}{1+\delta} \frac{K_2}{3!} (x^3 - 3xy^2)$$

$$x = \eta_x(s)\delta + x_\beta; K_2 = \frac{eS}{p_o c};$$

$$H = H_o + \Delta H_1 + \Delta H_{NL} \quad (16)$$

$$\Delta H_1 = -\delta \left((K_1 + K^2) \frac{x^2}{2} - K_1 \frac{y^2}{2} \right) + \delta \cdot \eta_x \cdot K_2 \frac{x_\beta^2 - y^2}{2}$$

$$\Delta H_{NL} = \frac{K_2}{3!} (x_\beta^3 - 3x_\beta y^2) + O(\delta^2);$$

We can calculate the linear chromaticity in the same fashion we deed above:

$$C_x = \frac{\Delta Q_x}{\delta} \cong -\frac{1}{4\pi} \oint \beta_x (K_1 + K^2 - \eta_x K_2) ds;$$

$$C_y = \frac{\Delta Q_y}{\delta} \cong \frac{1}{4\pi} \oint (\beta_y K_1 - \eta_x K_2) ds; \quad (17)$$

To zero chromaticities we should find distribution of sextupole fields (as function of s) such that that

$$\begin{aligned}\oint K_2(s)\eta_x(s)\beta_x(s)ds &= \oint \beta_x(s)\left(K_1(s)+K(s)^2\right)ds; \\ \oint K_2(s)\eta_x(s)\beta_y(s)ds &= \oint \beta_y(s)K_1(s)ds;\end{aligned}\tag{18}$$

Assuming positive dispersion (which is usual) it can be done by placing focusing sextupoles ($K_2 > 0$) in areas where β_x is large and β_y is small, and vice versa for defocusing quadrupoles with $K_2 < 0$. For most of know strong focusing lattices this can be done. The only exception is weak-focusing lattice where all terms are constants the compensation

$$\begin{aligned}\langle K_2 \rangle \eta_x &= (K_1 + K^2); \\ \langle K_2 \rangle \eta_x &= -K_1;\end{aligned}\tag{19}$$

could be possible only when $K_1 = -K^2 / 2$, which is exactly on the top the coupling resonances $Q_x = Q_y$. Hence, in general, in a weak-focusing storage ring chromaticity could be compensated only in one plane.

How the chromaticity compensation works: particle's average orbits shifts as function of energy and displacement is sextupoles generates effective gradient (quadrupole) field, which compensate change of the focusing from regular quadrupoles. This process is called feed-down – displacement of a high (n-th) order multipole generates lower orders multipoles, from dipole up to (n-1).

One important notion – compensating chromaticity requires orbit dependence on energy, which comes only as result of bending magnet. It means, that it is impossible to compensate chromaticity in a perfectly linear accelerator (no bends!) since transverse dispersion is always equal zero.

Thus, we established that in a modern storage rings chromaticity could be compensated using sextupoles. What is not obvious is that this can create significant problems. Indeed, modern light sources in order to generate high brightness beams reducing emittance (22-25)

$$\langle a_x^2 \rangle = \frac{55}{32\sqrt{3}} \gamma^2 \frac{\hbar}{mc} \frac{\left\langle |K|^3 \left((w_x \eta'_x - w'_x \eta_x)^2 + \left(\frac{\eta_x}{w_x} \right)^2 \right) \right\rangle}{(1 - \xi_{xy}) \langle K^2 \rangle}$$

strong focusing resulting in very large betatron tunes (~ 30) and very small beta-functions $\beta \sim R/Q$ and dispersion $\eta \sim R/Q^2$ measured in few cm. As follows from (17), we will need sextupole strength

$$\langle |K_2| \rangle \sim \langle |K_1| \rangle / \eta_x;$$

e.g. field inside the aperture of accelerator is very nonlinear and particle oscillating with large amplitudes can become unstable.

Since we introduced sextupoles, we should notice that equations of motion become non-linear. Even though the kick is locally proportional to a square of the transverse displacement, we cannot assume that it will generate some kind of expansion to a map of second order. One can simply observe that there is no analytical solution for equation of motion in a sextupole, or that two short sextupoles will already generate forth order terms in the transformations. Needless to say that multiple thick non-linear elements making the map tractable only by computers. But there is a BIG BUT – there is still a lot we can do to describe and to understand this nonlinear map – beyond just staring on them helplessly.

NSLS II arc lattice



First, let's discuss a simple case of a weak one-dimensional resonance. Let's in addition to our sextupole term introduce some octupole term – just to have a simple case of tune dependence on action (as you had seen in our previous lectures).

$$\Delta H_{NL} = \frac{K_2}{3!}(x^3 - 3xy^2) + \frac{K_3}{4!}(x^4 - 6x^2y^2 + y^4) \quad (16)$$

Again, we will use a simple parameterization uncouple linear motion:

$$x = \sqrt{2I_x\beta_x} \cos(\psi_x + \varphi_x); \quad y = \sqrt{2I_y\beta_y} \cos(\psi_y + \varphi_y);$$

to connect to action and angle Canonical variables. Just averaging the Hamiltonian (16) we get zero from sextupole term (outside resonances) and simple

$$\begin{aligned} \langle \Delta H_{NL} \rangle &= \left\langle \frac{K_3}{4!} \left(\frac{3}{2} \beta_x^2 I_x^2 - 6\beta_x\beta_y I_x I_y + \frac{3}{2} \beta_y^2 I_y^2 \right) \right\rangle; \\ \left\langle \frac{d\varphi_x}{ds} \right\rangle &= \frac{\langle K_3 \beta_x^2 \rangle}{8} I_x - \frac{\langle K_3 \beta_x \beta_y \rangle}{4} I_y; \quad \left\langle \frac{dI_x}{ds} \right\rangle = 0; \\ \left\langle \frac{d\varphi_y}{ds} \right\rangle &= \frac{\langle K_3 \beta_y^2 \rangle}{8} I_y - \frac{\langle K_3 \beta_x \beta_y \rangle}{4} I_x; \quad \left\langle \frac{dI_y}{ds} \right\rangle = 0; \end{aligned} \quad (17)$$

e.g. we have a well-defined dependence of the betatron tunes on their actions.

Similar dependence appears in the second order perturbation by sextupoles, which you could do using method we described in perturbation theory. For an accelerator it will give similar results with the same features, but slightly longer expressions. For the sake of going

further, we just acknowledge that there is tune dependence on amplitudes $\frac{\partial \mu_x}{\partial I_x} I_x$.

Now let's consider a case close to a third order resonance – with focus on x-direction – when $\mu_x = 2\pi \frac{N}{3} + \frac{\varepsilon}{C}; \varepsilon \ll 1$. The Hamiltonian

$$\begin{aligned} \Delta H_{NL} &= I_x^{3/2} \frac{\sqrt{2}K_2(s)}{3} \beta_x^{3/2}(s) \cos^3(\psi_x(s) + \varphi_x) + \frac{\partial \mu_x}{\partial I_x} \frac{I_x^2}{2} \\ \cos^3 \theta &= \frac{3}{4} \cos \theta + \frac{1}{4} \cos 3\theta; \quad \left\langle \frac{K_2}{3!} \beta_x^{3/2} \cos(\psi_x + \varphi_x) \right\rangle = 0; \\ \Delta H_{res} &= \frac{I_x^{3/2}}{6\sqrt{2}} \operatorname{Re} e^{3i(\varphi_x - \varepsilon/C)} f_3 + \frac{\partial \mu_x}{\partial I_x} \frac{I_x^2}{2}; \\ f_3 &= \left\langle K_2 \beta_x^{3/2} e^{3i(\psi_x + \varepsilon/C)} \right\rangle = \left\langle K_2 \beta_x^{3/2} e^{3i\chi_x} \cdot e^{6\pi i \frac{s}{C}} \right\rangle \end{aligned} \tag{18}$$

has now a resonant term, which is a third harmonic of the periodic function $K_2 \beta_x^{3/2} e^{3i\chi_x}$. Now we are ready to study this resonance, by including detuning into the phase using canonical transformation:

$$\begin{aligned} F &= - \left(\varphi_x + \frac{\varepsilon s}{C} + \arg f_3 \right) I; I = I_x; \varphi = \varphi_x + \frac{\varepsilon s}{C} + \arg f_3; \\ H_{res} &= \Delta H_{res} - \frac{\partial F}{\partial s} = \frac{I^{3/2}}{6\sqrt{2}} |f_3| \cos \varphi + \frac{\partial \mu_x}{\partial I_x} \frac{I^2}{2} + \frac{\varepsilon}{C} I. \end{aligned} \tag{19}$$

The beauty of this resonant form (this was the entire reason for all above manipulations) is that is s-independent. It means that trajectories in the phase space are simply contours of constant Hamiltonian. Let's first find stationary points:

$$H_{res} = \frac{I^{3/2}}{6\sqrt{2}}|f_3|\cos 3\varphi + \frac{\partial\mu_x}{\partial I_x} \frac{I^2}{2} + \frac{\varepsilon}{C} I \equiv \frac{a^3}{24}|f_3|\cos 3\varphi + \frac{\partial\mu_x}{\partial I_x} \frac{a^4}{8} + \frac{\varepsilon}{C} \frac{a^2}{2}$$

$$I' = -\frac{\partial H_{res}}{\partial \varphi} = \frac{I^{3/2}}{6\sqrt{2}}|f_3|\sin 3\varphi = 0 \rightarrow I = 0; \sin 3\varphi = 0; \varphi = \frac{n\pi}{3};$$

$$\varphi' = \frac{I^{1/2}}{4\sqrt{2}}|f_3|\cos 3\varphi + \frac{\partial\mu_x}{\partial I_x} I + \frac{\varepsilon}{C} = 0 \rightarrow \pm \frac{I^{1/2}}{4\sqrt{2}}|f_3| + \frac{\partial\mu_x}{\partial I_x} I + \frac{\varepsilon}{C} = 0.$$

with solutions at origin $I = 0$ and

$$\varphi = \frac{n\pi}{3}; n = 0, 1, \dots, 5; \frac{\partial\mu_x}{\partial I_x} I + (-1)^n \frac{I^{1/2}}{4\sqrt{2}}|f_3| + \frac{\varepsilon}{C} = 0;$$

$$2 \frac{\partial\mu_x}{\partial I_x} \cdot I^{1/2} = \sqrt{2} \frac{\partial\mu_x}{\partial I_x} \cdot a = (-1)^n \frac{|f_3|}{4\sqrt{2}} \pm \sqrt{\frac{|f_3|^2}{32} - 4 \frac{\partial\mu_x}{\partial I_x} \frac{\varepsilon}{C}};$$
(20)

with stationary points and their features depending on the sign and value of detuning. First, the resonance has a fixed width – the values under square root becomes negative when

$$\frac{|f_3|^2}{32} < 4 \frac{\partial\mu_x}{\partial I_x} \frac{\varepsilon}{C}$$
(21)

Depending on the sign of the $\frac{\partial \mu_x}{\partial I_x}$ it happens either at negative or positive detuning from the exact resonance, where three stationary stable points are located at amplitude of

$$a_o = \frac{1}{4} \left| \frac{f_3}{\mu'_x} \right|; I_o = \frac{1}{32} \left| \frac{f_3}{\mu'_x} \right|^2; \mu'_x \equiv \frac{\partial \mu_x}{\partial I_x} \quad (22)$$

while the point at zero is unstable – particles go around resonances. The plot below shows this on (φ, I) phase plot.

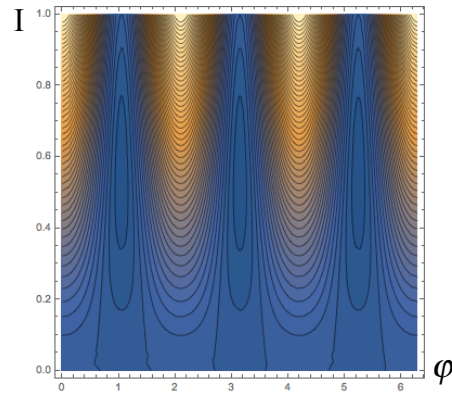


Fig.3. Phase plot at the exact 3rd order resonance.

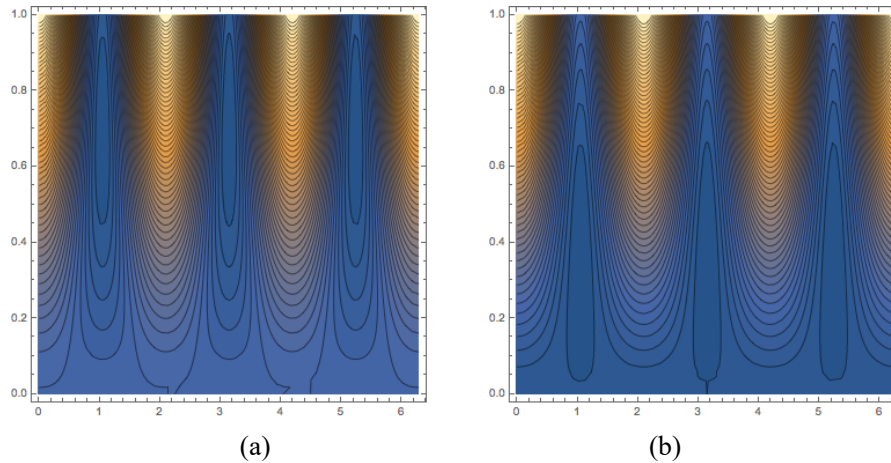


Fig.4. Phase plot at the exact 3rd order resonance for positive $\frac{\partial \mu_x}{\partial I_x}$; (a) below resonance, (c) above resonance, while islands exist. $I=0$ is stable point.

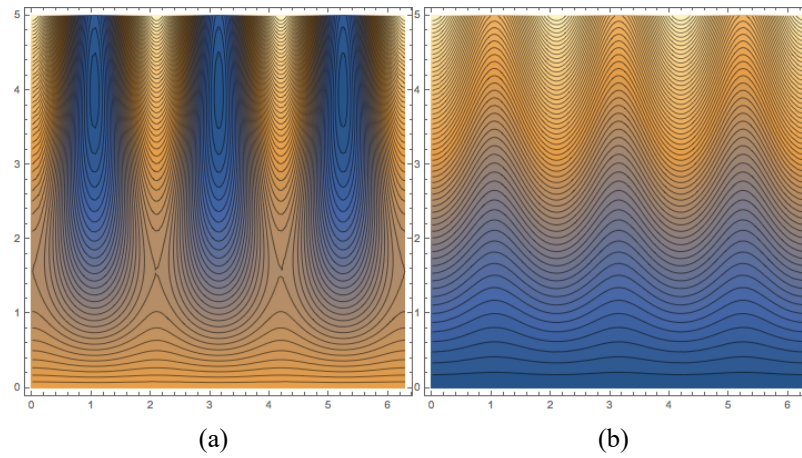


Fig.5. Phase plot at the exact 3rd order resonance for positive $\frac{\partial \mu_x}{\partial I_x}$; (a) below resonance islands still exists, (b) above resonance with conditions (21) satisfied, no islands. $I=0$ is stable point.

While the above plots are all correct, it is more informative to plot in polar coordinates $\{u = a \sin \varphi, v = a \cos \varphi\}$.

$$H_{res} = \frac{v^3 - 3vu^2}{24} |f_3| + \frac{\partial \mu_x}{\partial I_x} \frac{(u^2 + v^2)^2}{8} + \frac{\varepsilon}{C} \frac{u^2 + v^2}{2} \quad (23)$$

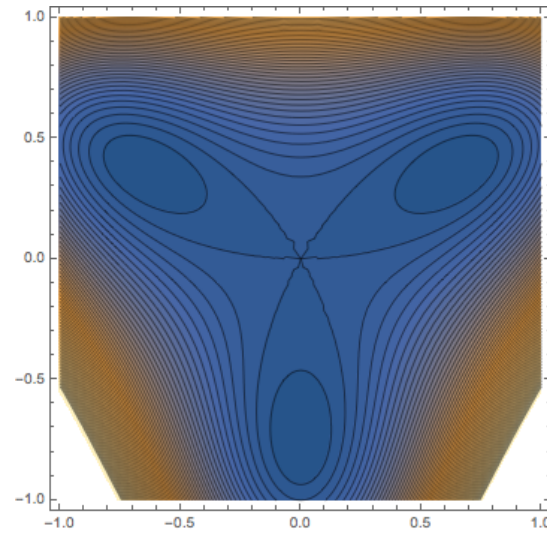


Fig.6. Phase plot at the exact 3rd order resonance.

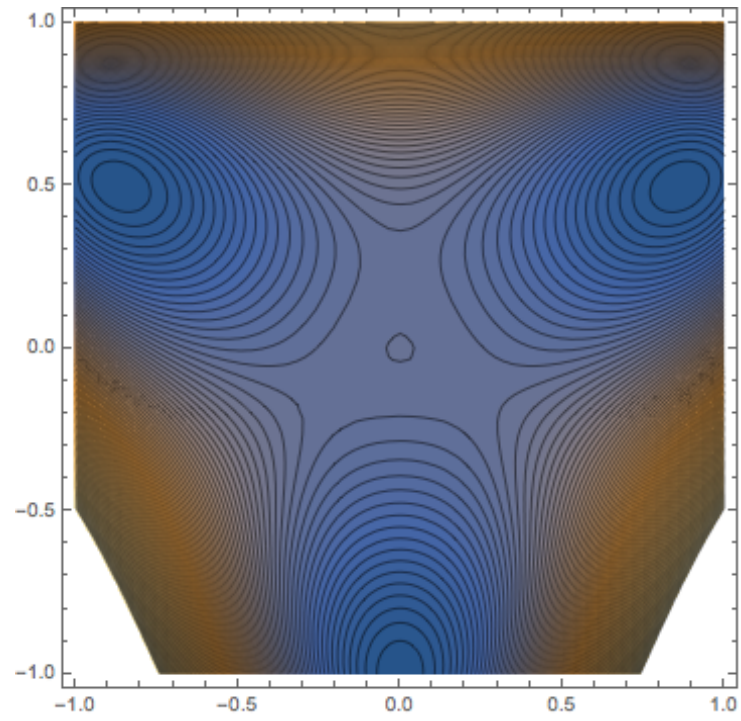


Fig.7. Phase plot below the 3rd order resonance.

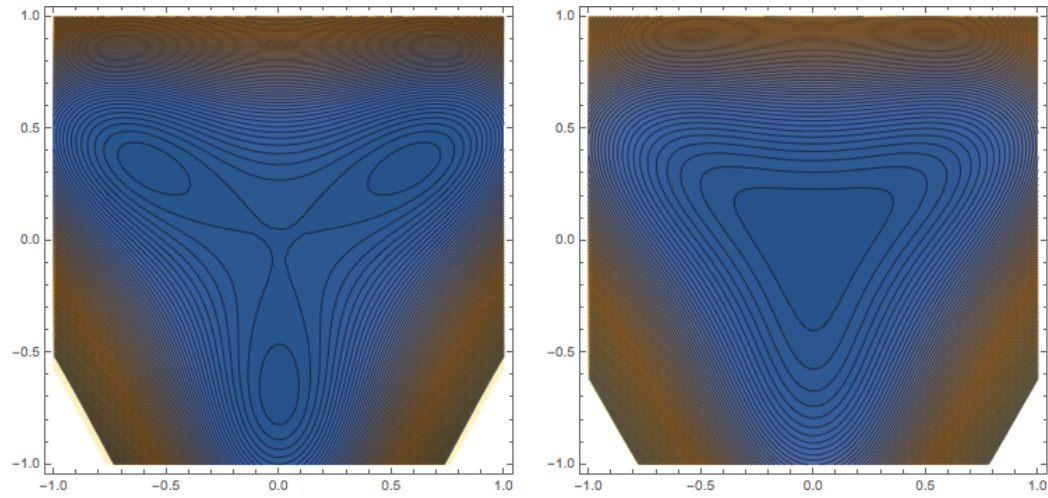


Fig.8. Phase plot above the 3rd order resonance. Left with islands, right without (e.g. outside the resonance band-width).

Similarly we could study resonances of higher orders, generated either by higher order multipoles or by higher orders perturbations from low order nonlinearities (sextupoles). Hamiltonian (16) already gives us plenty of possible resonances:

$$\begin{aligned}\Delta H_{NL} &= \frac{K_2}{3!}(x^3 - 3xy^2) + \frac{K_3}{4!}(x^4 - 6x^2y^2 + y^4) \\ x^3 &\rightarrow Q_x = n; 3Q_x = n; \quad xy^2 \rightarrow 2Q_y \pm Q_x = n; Q_x = n; \\ x^4 &\rightarrow 2Q_x = n; 4Q_x = n; \quad y^4 \rightarrow 2Q_y = n; 4Q_y = n; \\ &\quad x^2y^2 \rightarrow 2Q_y \pm 2Q_x = n.\end{aligned}\tag{24}$$

Coupling resonances are a bit more complicated to study – there are four variable and it is hard to plot 4D contour plots... But there is one interesting feature worth mentioning; let's consider a resonance $nQ_y \pm mQ_x = k$. It is easy to observe that resonance term in the Hamiltonian will have following forms

$$\begin{aligned}H_{res} &= f(I_x, I_y) \cos(n\varphi_x \pm m\varphi_y) \rightarrow \\ I'_x &= -\frac{\partial H_{res}}{\partial \varphi_x} = n \cdot f(I_x, I_y) \sin(n\varphi_x \pm m\varphi_y); \\ I'_y &= -\frac{\partial H_{res}}{\partial \varphi_y} = \pm m \cdot f(I_x, I_y) \sin(n\varphi_x \pm m\varphi_y); \\ \frac{d}{ds}(\pm mI_x - nI_y) &= 0 \rightarrow mI_x \mp nI_y = const\end{aligned}\tag{25}$$

which indicates that for difference coupling resonances, there is limitation on the possible amplitudes since $mI_x + nI_y = inv$. Meanwhile, the sum resonances do not impose such restriction and instead give us minimum values of the oscillation amplitudes since $mI_x - nI_y = inv$.

Sextupoles along generate in next order second, 4th and 6th order resonances in x, and a lot of coupling resonances (for example $mQ_y \pm nQ_x = k$; $n = 0, 2, 4; m = 2, 4$). You can continue building up the mountain of the resonances and to spice add the synchrotron motion and its tune into the picture. It seems that it does not matter what you do you will be close to some high order resonance. It became a practical matter what resonances have sufficient strength to mess-up life of realistic beam. As the matter of good practice, all resonances up to 4th order considered to be real killers (except difference linear coupling resonance $Q_x - Q_y = n$ which is even used to make beams round). Fig. 9 shows betatron tune resonance diagram below showing resonance for x-y betatron oscillations up to 4th order.

There is some settled difference between electron/positron storage rings, where damping by synchrotron radiation effectively destroy weak resonances, and hadron storage rings/colliders where damping is either weak or practically negligible. The later are trying to stay away also from 5th and 6th order resonances as a good practice. Qualitatively resonances are described by their strength, which can be measured/estimated by the oscillating frequency (tune) inside the resonate separatrix (island). For example, we can calculate what will be the oscillation frequency inside separatrix (island) in Fig. 6 (exactly at 3rd order resonance) by expanding Hamiltonian around stationary point:

$$\begin{aligned}
 I_o &= \frac{a_o^2}{2} = \frac{1}{32} \left| \frac{f_3}{\mu'_x} \right|^2; a_o = \frac{1}{4} \left| \frac{f_3}{\mu'_x} \right|; \cos 3\varphi = \pm \left(1 - \frac{9\varphi^2}{2} \right) \dots \\
 I^{3/2} &= I_o^{3/2} + \frac{3}{2} I_o^{1/2} \delta I + \frac{3}{8} I_o^{-1/2} \delta I^2 \dots; I^2 = I_o^2 + 2I_o \delta I + \delta I^2; \\
 &\pm \left(1 - \frac{9\varphi^2}{2} \right) \frac{a_o^{3/2}}{24} |f_3| \pm \frac{|f_3|}{6\sqrt{2}} \left(\frac{3}{2} \sqrt{I_o} \delta I + \frac{3}{8} \frac{\delta I^2}{\sqrt{I_o}} \right) + \frac{\mu'_x}{2} (I_o^2 + 2I_o \delta I + \delta I^2) \\
 &\pm \frac{|f_3|}{6\sqrt{2}} \frac{3}{2} \sqrt{I_o} + \mu'_x I_o = \pm \frac{|f_3|}{32} \left| \frac{f_3}{\mu'_x} \right| + \mu'_x \frac{1}{32} \left| \frac{f_3}{\mu'_x} \right|^2 = 0; \\
 H_{sep} &= \frac{\mu'_x}{2} \left(\frac{3\varphi^2}{2} \left| \frac{f_3}{4\mu'_x} \right|^4 + \frac{\delta I^2}{2} \right); \Omega = \sqrt{3} \left| \frac{f_3}{4\mu'_x} \right|^2;
 \end{aligned}$$

The frequency of oscillation is the measure of the damping rate required to destroy such separatrix (island).

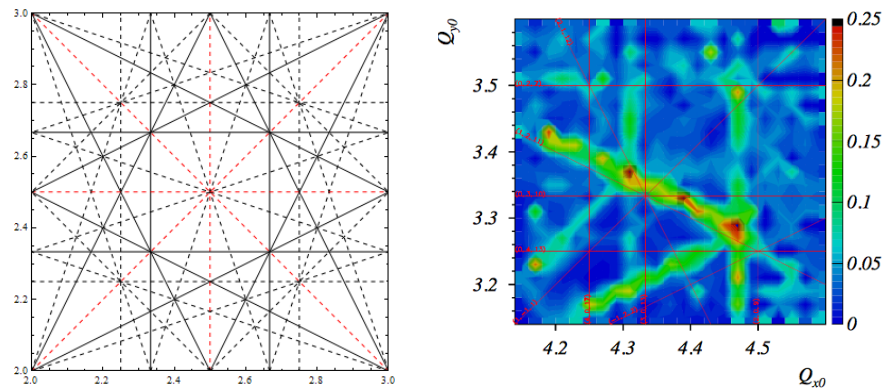


Fig.9. A resonant tune diagram (above, for an arbitrary storage ring) and rate of particle losses in SIS18 storage ring (right)

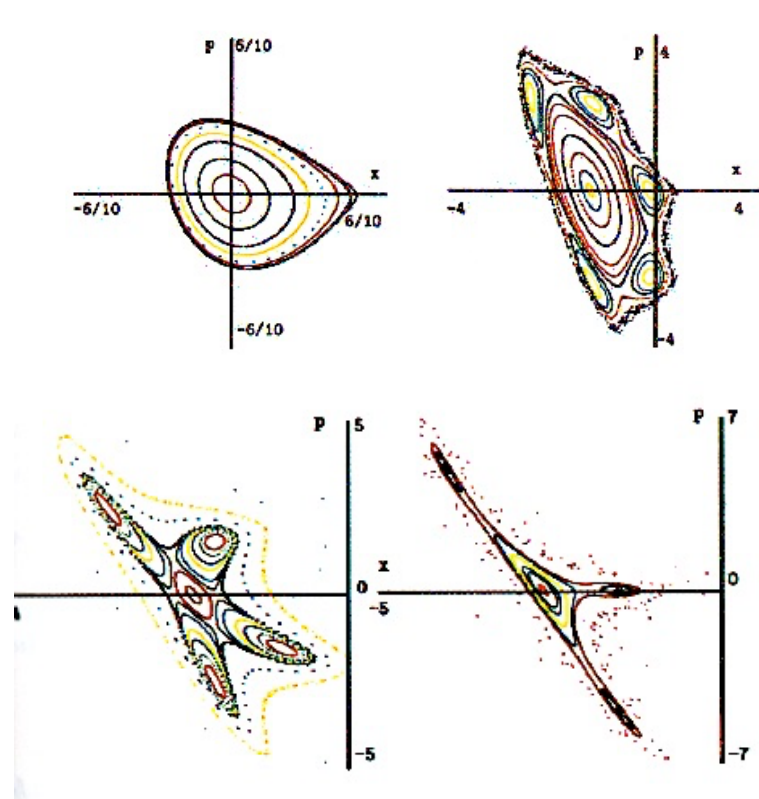


Fig.10. Set of non-linear maps with typical characteristics of first order, 5th order, 4th order and 3rd order resonances (taken from E. Forset, Beam Dynamics).

The next effect, which is important, is stochastic trajectories, which appear in the motion of the particles (turn by turn) – see Fig. 11. One of a simple criteria which was developed is called Chirikov criteria, stating that that stochastic layer in Poincare diagrams (the particles motion) appears when two non-linear resonances overlap. Careful look into fig 11 reveals that in addition to main resonance (4th and 3rd order) there are additional high order resonance (islands) formed – some of them clearly identifiable, some destroyed and turned into a stochastic layer. Usually stochastic layer cause loss of particles at large amplitudes. It is also typical (with exception of beam-beam effects, when the nonlinearity of the beam is of the order of the beam size) that motion at large amplitudes becomes unstable and chaotic. Area of the dynamically (not physically) stable motion of particles is called “dynamic aperture” or DA.

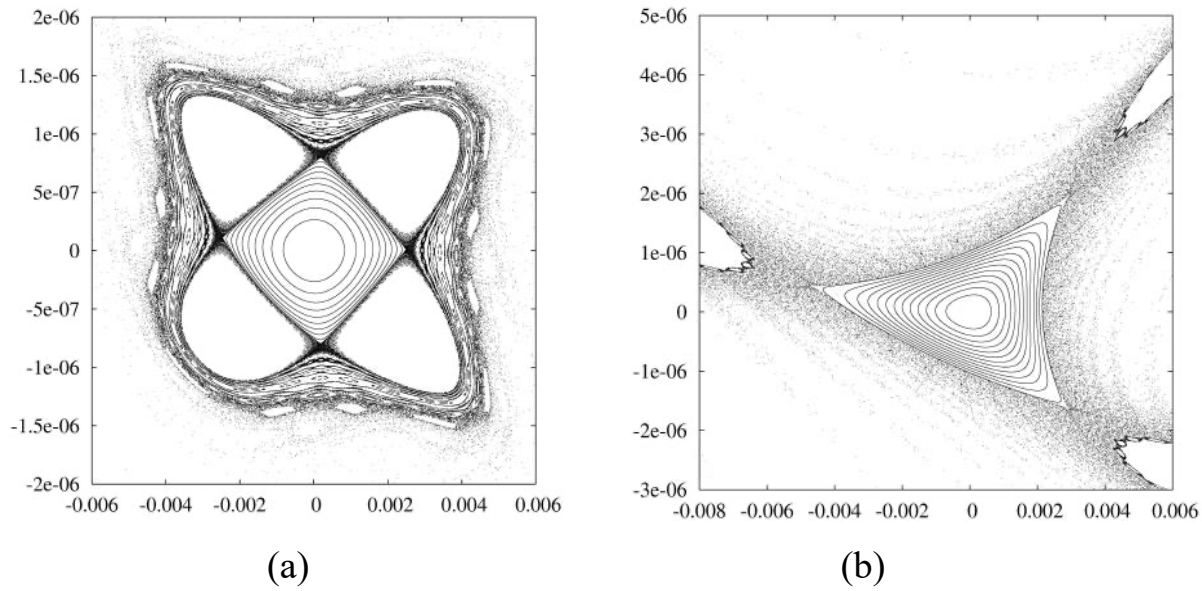


Fig.11. Two tracking results: (a) with 4th order and (b) 3rd order resonance strictures.

Methods of increasing dynamic aperture are multiple and there is no one specific trick (or set of tricks), which does the magic – to a degree it remains to be an art form. Still, reducing strength of the resonant terms and low order geometrical distortion are necessary steps in creating modern accelerator with large dynamic aperture.

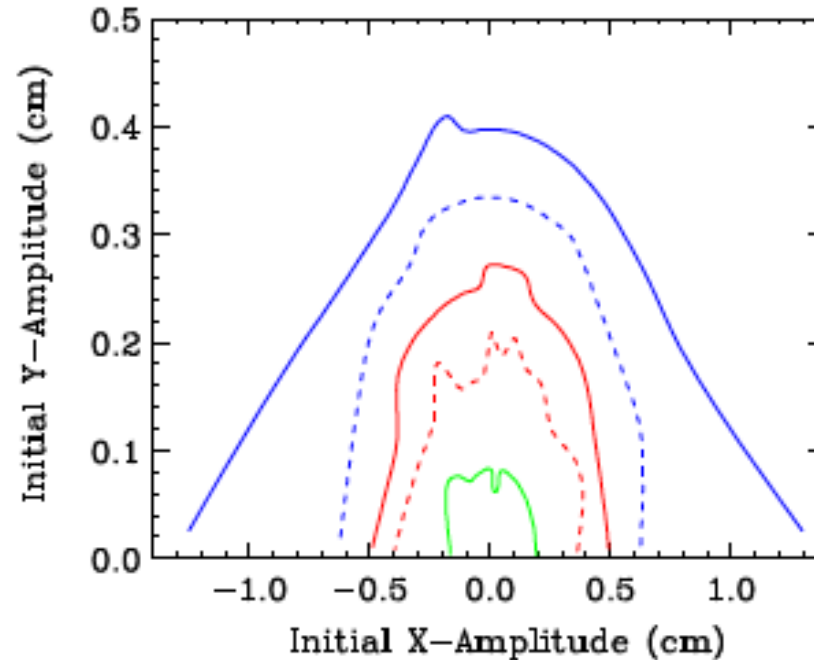


Fig.12. Momentum dependent dynamic aperture for 4th-order geometrical achromat (with zero chromaticity) Energy offsets: 0% - blue solid, 0.5% - dashed blue, 1% - red solid, 1.5% - dashed red, 1.5% - green. The dynamic aperture shown in a specific place in the storage ring – particles launched outside the dynamic aperture do not survive and are lost at large amplitudes.

Computers playing important role in both generating and analyzing non-linear maps. There is a very strong link to cosmology, which faces problems similar to that in modern accelerators - a long-time tracking of solar and star systems. One the modern tools in DA studies is borrowed from cosmology and called frequency map analysis (FMA) – the idea is to characterize how chaotic is the motion of particles with given amplitude of oscillations.

If we perform a discrete Fourier transform on the tracking data (starting with an initial x-y) position and obtain the betatron tunes (for N turn tracking, the precision is 1/N). If we repeat this process with different initial positions, we can obtain a tune map. To indicate the variation of the tunes over different turns of the ring, we can define a diffusion or regularity, which describes the difference between the tunes over various periods (usually the first half of the tracking (Q_{x1} , Q_{y1}) and the second half (Q_{x2} , Q_{y2})). In other words, we define a diffusion constant D:

$$D = \log_{10} \sqrt{(Q_{y2} - Q_{y1})^2 + (Q_{x2} - Q_{x1})^2} .$$

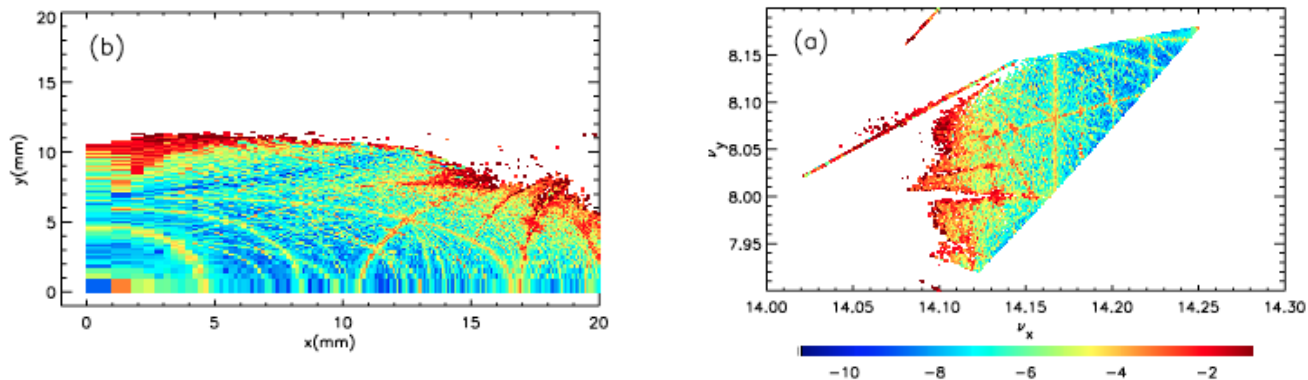


Fig. 13. The frequency map for an ideal lattice for ALS light source (LBNL) in tune space (a) and real space (b). The color scheme is logarithmic, with blue indicating completely stable motion and red/dark red chaotic behavior close to complete loss of stability (white).

It only looks scary – in reality, we always find location in the Q-map to operate storage rings

